ACS Catalysis

Research Article

pubs.acs.org/acscatalysis

Design of Organocatalysts for Asymmetric Propargylations through Computational Screening

Analise C. Doney,[†] Benjamin J. Rooks,[‡] Tongxiang Lu,[§] and Steven E. Wheeler*

Department of Chemistry, Texas A&M University, College Station, Texas 77842, United States

Supporting Information

ABSTRACT: The development of asymmetric catalysts is typically driven by the experimental screening of potential catalyst designs. Herein, we demonstrate the design of asymmetric propargylation catalysts through computational screening. This was done using our computational toolkit AARON (automated alkylation reaction optimizer for *N*-oxides), which automates the prediction of enantioselectivities for bidentate Lewis base catalyzed alkylation reactions. A systematic screening of 59 potential catalysts built on 6 bipyridine *N*,*N*′-dioxide-derived scaffolds results in predicted ee values for the propargylation of benzaldehyde ranging from 45% (*S*) to 99% (*R*), with 12 ee values exceeding 95%. These data provide a broad set of experimentally testable predictions. Moreover, the associated data revealed key details regarding the role of stabilizing electrostatic interactions in asymmetric propargylations, which were harnessed in the design of a propargylation catalyst for which the predicted ee exceeds 99%.

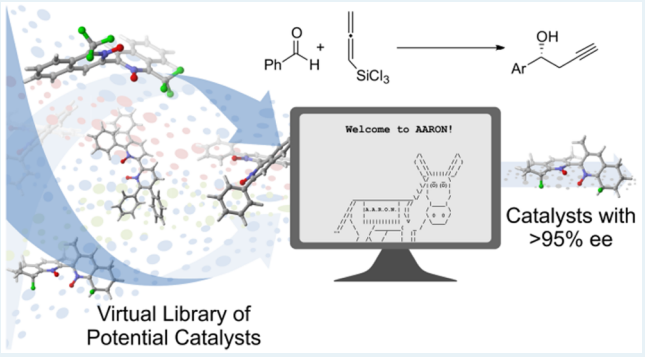

KEYWORDS: *computational design, stereoinduction, electrostatics, steric interactions, density functional theory, noncovalent interactions*

I. INTRODUCTION

Computational quantum chemistry has matured considerably over the past decade, and applications of modern density functional theory (DFT) methods have provided reliable mechanistic insights into myriad organocatalyzed reactions.[1] However, the computational design of asymmetric organocatalysts remains a significant challenge,[2] and new catalysts are still typically developed on the basis of the experimental screening of potential catalyst designs. The primary reason is the considerable time, effort, and expertise required to accurately compute the relative energies of all thermodynamically accessible stereocontrolling transition state (TS) structures using DFT, which makes it much more efficient to experimentally test a library of potential catalysts than to screen them computationally.

A number of strategies have been proposed to upend this paradigm. For instance, transition state force fields (TSFFs) have a long history[3] and can enable the rapid screening of catalyst designs with remarkable accuracy.[4] We have taken a different approach,[1f] developing a computational toolkit (AARON: automated alkylation reaction optimizer for *N*-oxides)[5] that automates the DFT optimization of all required TS structures needed to predict enantioselectivities for bidentate Lewis base catalyzed alkylation reactions.[5,6] This has opened the door to the screening of potential catalysts for these reactions using quantum mechanics.

Lewis base promoted alkylation reactions, developed by Kobayashi et al.[7] and Denmark and co-workers[8] in the early 1990s, offer transition-metal-free routes to key chiral building blocks. Nakajima et al.,[9] as well as others,[10] have demonstrated the utility of axially chiral bipyridine *N*-oxides and *N*,*N*′-dioxides in Lewis base promoted allylation reactions. However, the development of similar catalysts for asymmetric propargylations using allenyltrichlorosilanes has proved much more challenging (reaction 1, Scheme 1).[9b,11] For instance, Nakajima et al.[9] showed that **4a** (Scheme 2, R = Me) catalyzes both the allylation and propargylation of benzaldehyde.[12] However,

Scheme 1. Asymmetric Propargylation of Benzaldehyde using Allenyltrichlorosilane, along with a Depiction of the Stereocontrolling Step

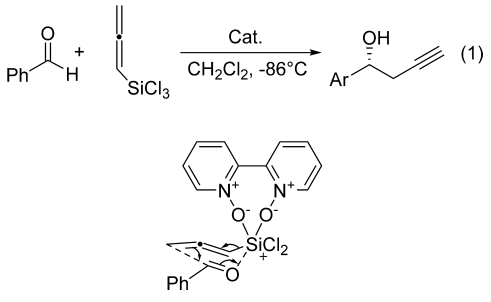

Received: August 18, 2016
Revised: October 7, 2016
Published: October 14, 2016

DOI: 10.1021/acscatal.6b02366
ACS Catal. 2016, 6, 7948−7955

Scheme 2. Library of Catalysts That Were Screened for Reaction 1

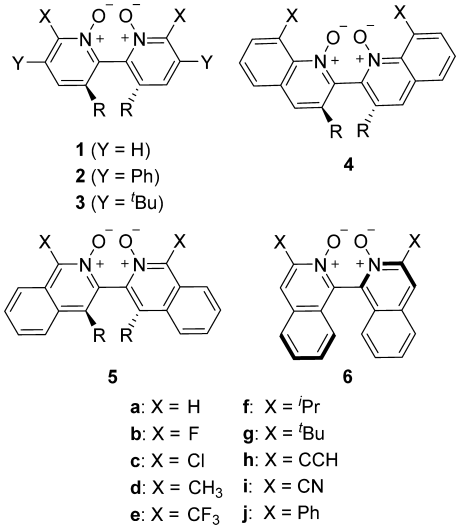

whereas the reported ee for the allylation was 88%,[9a] the ee for the propargylation under similar reaction conditions was only 52%.[9b] The first highly enantioselective transition-metal-free propargylation catalyst was not developed until 2013, when Takenaka and co-workers[11b] developed a helical bipyridine *N*-oxide catalyst that provides the homopropargylic alcohol in 86% ee.[13]

There has been considerable work elucidating the mechanism and origin of enantioselectivity in bipyridine *N*-oxide and *N*,*N*′-dioxide catalyzed allylation and propargylation reactions.[9a,10f,14] In solvents such as dichloromethane, the stereocontrolling step involves a closed, chairlike TS built around a hexacoordinate silicon intermediate (see Scheme 1).[9a,14] Sepúlveda and co-workers[12] showed that, for C_2-symmetric catalysts, there are 5 possible ligand arrangements around this hexacoordinate silicon (see Figure 1). These give

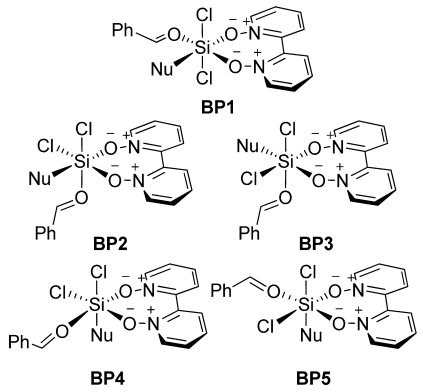

Figure 1. Five distinct ligand configurations for C_2-symmetric bidentate Lewis base catalyzed alkylation reactions, where Nu is the alkyl nucleophile.

rise to 10 distinct structures for this stereocontrolling TS (for each of the 5 ligand configurations, the alkyl nucleophile can add to either face of benzaldehyde).[6] While any of these TS structures can in principle be thermodynamically accessible for a given catalyst, we have found that TS structures based on ligand configurations BP1, BP2, and BP3 are most likely to be low-lying.[6]

In 2015, Rooks et al.[6] used AARON to predict the enantioselectivities of 18 previously reported bipyridine *N*,*N*′-dioxide catalysts for the allylation of benzaldehyde. The data revealed that ee values predicted at the B97-D/TZV(2d,2p) level of theory exhibit a mean absolute error of 13% ee in comparison to experiment. This corresponds to an error in Boltzmann weighted relative barrier heights of only 0.25 kcal mol^{-1} (see Table S1 in the Supporting Information) and suggests that the same computational approach should be reliable when applied to propargylations. On the basis of this, Rooks et al.[6] also predicted ee values for these 18 catalysts applied to the propargylation of benzaldehyde. Two catalysts showed promising ee values (including catalyst **6j**; Scheme 2),[10g] and Rooks et al.[6] argued that bipyridine *N*,*N*′-dioxides provide a promising platform for the development of highly enantioselective propargylation catalysts.

Motivated by these results,[6] we have used AARON to screen a virtual library of bipyridine *N*,*N*′-dioxide derivatives for the propargylation of benzaldehyde using allenyltrichlorosilane (Scheme 2), revealing a dozen catalysts for which predicted ee values exceed 95%. Analyses of the predicted enantioselectivites and associated TS structures reveal that high ee values can be achieved by tuning the electrostatic environment of the formyl C−H of benzaldehyde. The power of this strategy is demonstrated through the design of a novel bipyridine *N*,*N*′-dioxide that is predicted to provide an ee exceeding 99%.

II. THEORETICAL METHODS

All computations were performed at the B97D/TZV(2p,2d) level of theory,[15] accounting for solvent effects (dichloromethane) using the polarizable continuum model (PCM).[16] This level of theory has proved reliable for *N*-oxide and *N*,*N*′-dioxide catalyzed allylations and propargylations, in comparison to both experimental selectivities and high-accuracy ab initio data.[6,11a,12,13] For each catalyst considered, we optimized the 10 possible TS structures arising from the 5 distinct ligand configurations in Figure 1. Transition state structures were confirmed on the basis of harmonic vibrational frequency analyses. Predicted ee values were derived from a Boltzmann weighting of relative energy barriers at 195 K,[13] which is based on the assumption that these reactions are under Curtin−Hammett control. For catalysts built on scaffold **2**, multiple low-lying conformers are possible for some of the 10 distinct TS structures (see the Supporting Information). These conformers were also optimized and accounted for in the Boltzmann weighting. Previous work on allylation reactions has shown that relative energy barriers at this level of theory provide more robust predictions of ee values than do free energies.[6] As such, ee values derived from relative TS energies are presented below; predicted ee values based on relative enthalpies, RRHO free energies, and quasi-RRHO free energies[17] are provided in Table S2 in the Supporting Information. For all of the catalysts for which the predicted ee values exceed 95% on the basis of relative energy barriers, the corresponding predictions from relative enthalpies or quasi-RRHO free energies are similar.

The construction and optimization of all TS geometries were facilitated by AARON,[5] which has been described previously.[1f,6] AARON provides an interface to Gaussian 09,[18] which was used to carry out all DFT optimizations. Density fitting techniques were used throughout. Below, TS structures are named on the basis of the arrangement of ligands around the hexacoordinate silicon (see Figure 1) and whether the TS leads

DOI: 10.1021/acscatal.6b02366
ACS Catal. 2016, 6, 7948−7955

to formation of the (*R*)- or (*S*)-alcohol. For example, BP2(*R*) will refer to the TS structure leading to the (*R*)-alcohol in which the ligand configuration corresponds to that in BP2.

III. RESULTS AND DISCUSSION

Catalyst scaffolds **1**−**6** represent six classes of bipyridine-*N*,*N*′-dioxide derivatives. The parent scaffold, **1**, is an (*S*)-2,2′-bipyridine *N*,*N*′-dioxide with substituents (X) at the 6,6′-positions. Catalysts **2** and **3** include additional Ph or ^{t}Bu substituents (Y) at the 5,5′-positions, respectively. Scaffold **4** is an (*S*)-8,8′-disubstituted 2,2′-biquinoline *N*,*N*′-dioxide, **5** is an (*S*)-1,1′-disubstituted 3,3′-biisoquinoline *N*,*N*′-dioxide, and **6** is an (*S*)-3,3′-disubstituted 1,1′-biisoquinoline *N*,*N*′-dioxide. Among these catalysts, examples built on scaffolds **1**, **4**, and **6** have previously been synthesized and used as catalysts for asymmetric allylations.[9,10b,g] To our knowledge, only catalyst **4a** has been tested for reaction 1 (Scheme 1), for which Nakajima and co-workers[9b] reported an ee of 52% in 2002.[19] Scaffold **5**, which features a relatively uncommon 1,1′-biisoquinoline connectivity, has not previously been explored as an organocatalyst; however, derivatives of **5d** have been synthesized previously for other purposes.[20] Thus, nearly all of the catalysts in Scheme 2 should be synthetically viable. We note, however, that some are highly sterically congested (e.g., **3e**−**g**), and their syntheses might be nontrivial as a result. Regardless, the computational consideration of these catalysts provides additional insight into the effect of different groups on the predicted enantioselectivity.

Experimentally, the substituent R in scaffolds **1**−**5** must be sufficiently bulky to prohibit catalyst racemization. However, this is unnecessary computationally, since the axial chirality of the catalyst can be fixed during the initial geometry optimizations. To probe whether the identity of R impacts the enantioselectivity, we compared predicted ee values for catalysts **1a**−**6a** with R = H, CH_3 (see Table 1). The predicted ee values for R = H are qualitatively similar to those for the more realistic catalysts with R = Me. As such, in order to eliminate problems associated with converging to TS structures for simple methyl rotations, rather than the targeted stereocontrolling transition state, we have considered R = H for the sake of screening the catalyst library shown in Scheme 2; R = Me was then tested for the catalysts for which the predicted ee values exceed 95% (see Table S3 in the Supporting Information).

Table 1. Predicted ee Values for Reaction 1[a]

Cat.	1	2	3	4	5	6
a (R = Me)	69	74	67	54[b]	76	-
a	76	83	54	24	78	73
b	89	94	**97**	71	90	89
c	91	**96**	**97**	75	92	91
d	65	77	83	-45	79	58
e	94	**99**	**97**	18	**97**	**96**
f	71	-10	90	-28	86	63
g	25	-18	c	75	47	-31
h	86	**97**	**97**	52	92	91
i	93	**99**	**99**	88	**96**	94
j	41	91	30	87	45	88

[a]R = H, except where noted. Positive ee values correspond to excess (*R*)-alcohol formation, whereas negative values indicate excess (*S*)-alcohol. These ee values are based on relative energy barriers. Values based on relative enthalpy and free energy barriers are available in Table S2 in the Supporting Information. [b]Experimental ee 52%.[9b] [c]Catalyst **3g** is too sterically encumbered to be viable.

Predicted ee values for 59 of the 60 catalysts (R = H) are shown in Table 1; catalyst **3g** was too sterically crowded to compute viable TS structures. The relative energies of the low-lying TS structures are plotted in Figure 2 (see the Supporting Information for complete data). These plots emphasize the sheer quantity of thermodynamically accessible TS structures for these catalysts, highlighting both the necessity of accounting for a Boltzmann weighted ensemble of TS structures and the overall difficulty of designing highly enantioselective catalysts for this transformation. In order to achieve high degrees of enantioselectivity, there must be a significant energy gap between the lowest-lying TS(*R*) and all of the (*S*)-transition states.

Overall, catalysts **1a**−**6a** show modest enantioselectivities for the propargylation of benzaldehyde (see Table 1). However, the introduction of substituents onto these scaffolds results in drastic changes in the predicted enantioselectivities, with ee values ranging from 45% (*S*) to 99% (*R*). Ultimately, 12 catalysts were predicted to yield ee values exceeding 95%. For these 12 catalysts, predictions for R = Me are provided in Table S3 in the Supporting Information. In each case, the replacement of H with Me results in no substantial change in the predicted ee.

The predicted ee values of these catalysts can be compared with those of the parent catalyst, **1a**. In **1a**, the 0.9 kcal mol^{-1} energy difference between BP2(*S*) and BP2(*R*) has previously been attributed to favorable electrostatic interactions between the formyl C−H of the benzaldehyde and one of the chlorines bound to silicon (see Figure 3);[13] this interaction is absent in BP2(*S*). This preferential electrostatic stabilization of BP2(*R*) over BP2(*S*) can be seen explicitly by comparing the electrostatic potential (ESP)[21] of the catalyst in the plane of the formyl group in these two TS structures (see Figure 3). These ESPs show that the partially positively charged C−H group[22] is in a much more favorable electrostatic environment in BP2(*R*) than it is in BP2(*S*). We note that this inherent electrostatic stabilization of BP2(*R*) is present to a similar degree for all of the catalysts considered, and the differences in enantioselectivities arise primarily from effects that alter the distribution of the other TS energies relative to BP2(*R*). Echoing previous findings from Rooks et al.,[6] BP2(*R*) is the lowest-lying (*R*)-transition state for 57 of the 59 catalysts considered. Similarly, BP2(*S*) is the lowest-lying (*S*)-transition state for 48 of the catalysts.

Several broad trends emerge from the data in Table 1. First, catalysts built on scaffold **4** tend to be outliers, exhibiting ee values that are drastically different from those of the other five scaffolds for a given substituent. This is unsurprising given the different placement of the substituents X on scaffold **4** relative to the reaction center, in comparison to the other scaffolds. Moreover, none of the catalysts built on scaffold **4** are predicted to provide high enantioselectivities. Excluding **4**, the substituent effects on the predicted ee values are qualitatively similar across the different scaffolds, with the exception of isopropyl (**f**) and phenyl (**j**) substituents. The introduction of ^{i}Pr groups leads to highly varied ee values, which appear to result from the steric demands of the iPr groups. For some catalyst scaffolds, the introduction of these bulky groups destabilizes low-lying competing TS structures, enhancing the enantioselectivity in comparison to the unsubstituted cases; in other instances, these interactions destabilize the BP2(*R*) and lead to low ee values. In

DOI: 10.1021/acscatal.6b02366
ACS Catal. 2016, 6, 7948−7955

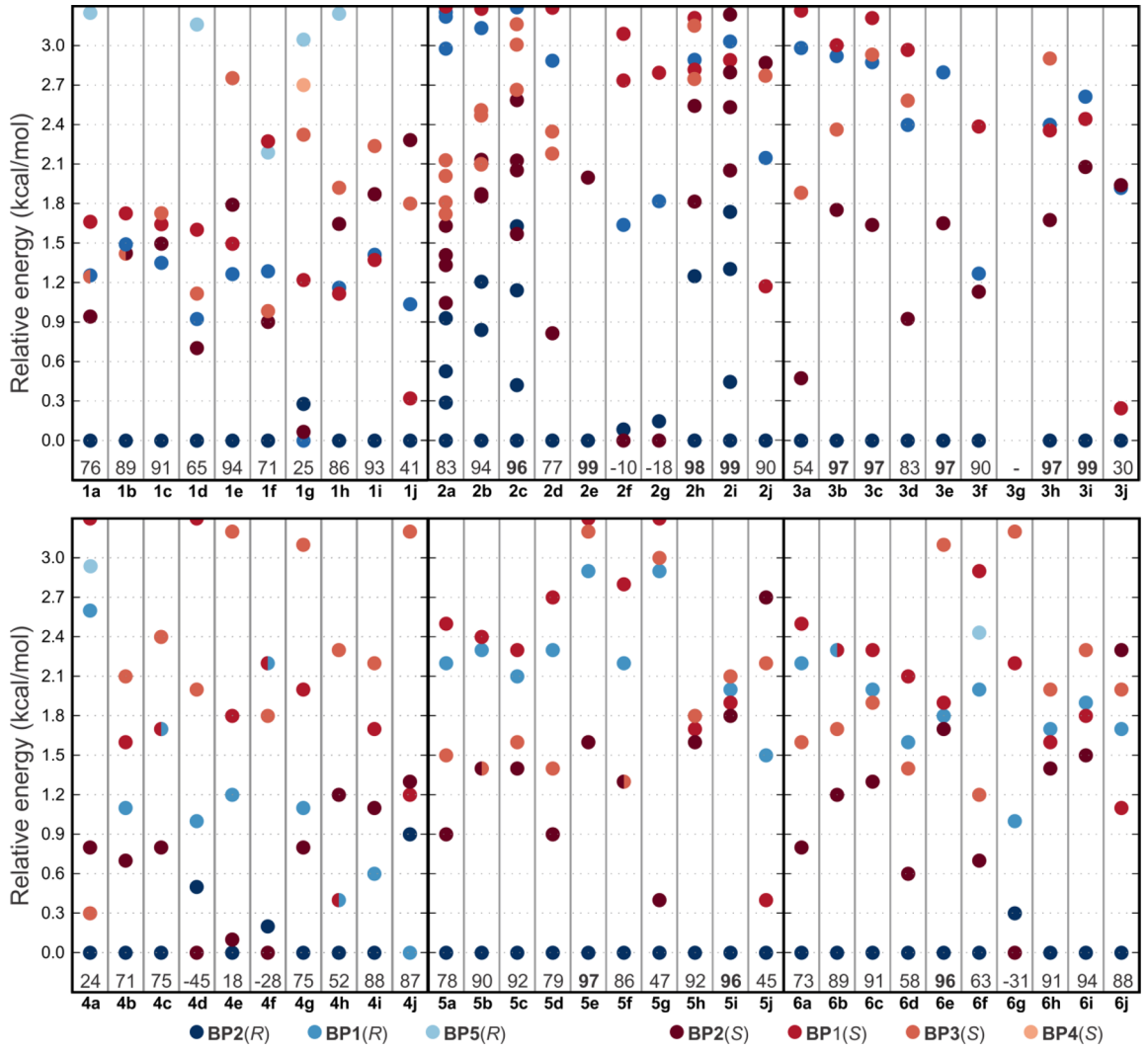

Figure 2. B97-D/TZV(2d,2p) predicted relative energies (kcal mol^{-1}) of the thermodynamically accessible TS structures for catalysts **1a**–**6j** (N.B.: for **2a**–**j**, there are multiple low-lying conformers for some of the TS structures corresponding to different orientations of the phenyl rings).

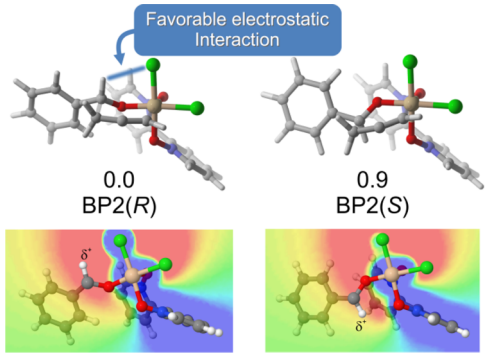

Figure 3. Key TS structures for catalysts **1a** along with relative energies in kcal mol^{-1}. Also displayed are the ESPs of the catalyst in the plane of the formyl group (red, −30 kcal mol^{-1}; blue, +30 kcal mol^{-1}; allenyl group removed for clarity).

these cases, the predicted ee values resemble those for *tert*-butyl substituents (**g**), which are uniformly much lower than those for the corresponding unsubstituted catalysts. For instance, the introduction of ^{t}Bu substituents changes the 83% (*R*) predicted ee for **2a** to 18% (*S*) for **2g**. Similarly, whereas **6a** is predicted to provide an ee of 73% (*R*), the ee for **6g** is predicted to be 31% (*S*). These reduced ee values for the ^{t}Bu-substituted catalysts result from the destabilization of BP2(*R*) through steric interactions. For example, for **1g** (predicted ee 25%; see Figure 4), unfavorable steric interactions between one of the *tert*-butyl substituents and the formyl C−H in BP2(*R*) overwhelm the stabilizing effects from favorable C−H···Cl interactions. As a result, BP2(*R*) is actually higher in energy than BP2(*S*) in this case.[23]

The impact of phenyl substituents (**j**) are even more intriguing, with predicted ee values either being relatively high (91, 87, and 88% ee for **2j**, **4j**, and **6j**, respectively) or much more modest (41, 30, and 45% ee for **1j**, **3j**, and **5j**, respectively). With the exception of **4j** (which, again, is an outlier), the predicted ee of the Ph-substituted catalysts hinges on the energy of BP1(*S*) relative to BP2(*R*); BP2(*S*) is relatively high in energy and does not strongly affect the ee values of these catalysts. For the nonselective Ph-substituted catalysts, favorable π-stacking and CH/π interactions[24] preferentially stabilize BP1(*S*), degrading the enantioselectivity. For instance, the 41% ee predicted for **1j** can be attributed to the π-stacking and CH/π interactions that stabilize BP1(*S*), but not BP2(*R*) (see Figure 4). The result is that BP1(*S*) in only 0.3 kcal mol^{-1} higher in energy than BP2(*R*). In the case of the

DOI: 10.1021/acscatal.6b02366
ACS Catal. 2016, 6, 7948−7955

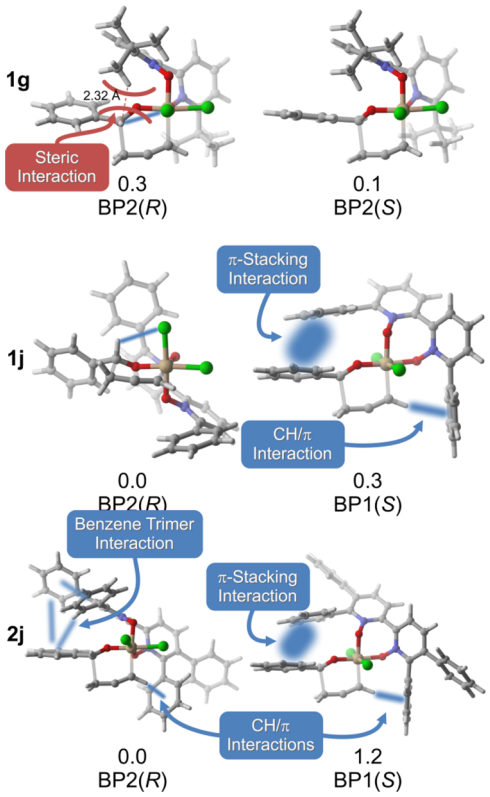

Figure 4. Key TS structures for catalysts **1g**,**j** and **2j** along with relative energies in kcal mol^{-1}. BP1(R), which is low-lying for **1g**, is not pictured.

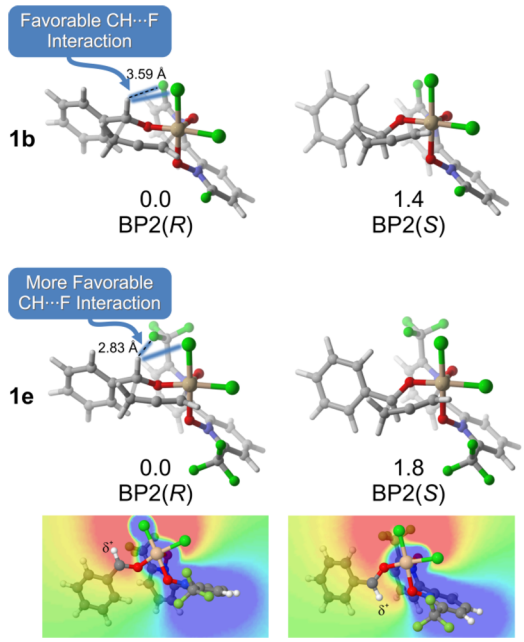

Figure 5. Key TS structures for catalysts **1b**,**e** along with relative energies in kcal mol^{-1}. For **1e**, the electrostatic potential of the catalyst in the plane of the formyl group of benzaldehyde is also plotted (red, −30 kcal mol^{-1}; blue, +30 kcal mol^{-1}; allenyl group removed for clarity).

selective Ph-substituted catalysts, there are additional π-stacking interactions favoring BP2(R). For example, for **2j** (predicted ee 90%; see Figure 4), a benzene trimer like interaction[25] involving the benzaldehyde and two Ph substituents on the catalyst is present in BP2(R), offsetting the π-stacking and CH/π interactions that favor BP1(S). Similar interactions are at play among the benzaldehyde, naphthyl backbone, and phenyl substituent of **6j** (predicted ee 88%). These data add to recent examples where the ee of a given organocatalytic transformation can rise or fall due to the subtle interplay of favorable noncovalent interactions in competing TS structures.[1f,26]

The effect of other substituents is more uniform across the different scaffolds (excluding **4**), resulting in qualitatively similar trends in predicted ee values in comparison to the corresponding unsubstituted catalysts. For instance, the introduction of fluoro (**b**) or chloro (**c**) substituents enhances the predicted enantioselectivity, with the effect of Cl being slightly greater than that of F. These enhanced ee values can be attributed to the introduction of stabilizing C−H···X (X = F, Cl) interactions between the halogen substituent and the formyl C−H of the benzaldehyde. For instance, for **1b** the fluoro substituent is 3.59 Å from the formyl C−H in BP2(R), contributing to the 1.4 kcal mol^{-1} energy difference between BP2(S) and BP2(R) (see Figure 5).[27] Methyl (**d**) and trifluoromethyl (**e**) substituents also have a similar effect across these scaffolds, with Me generally leading to lower selectivities and CF_3 to higher selectivities in comparison to the corresponding unsubstituted catalysts. The former effect is a result of the stabilization of BP2(S), relative to BP2(R). The latter effect arises from favorable C−H···F interactions that stabilize BP2(R) but not BP2(S). For example, for **1e**, one of the fluorines of the CF_3 group is only 2.89 Å from the formyl C−H (see Figure 5). This distance is considerably shorter than that in catalyst **1b**, and the effect on the electrostatic environment of the formyl C−H group in BP2(R) and BP2(S) is correspondingly greater (see Figure 5). The result is a substantial 1.8 kcal mol^{-1} energy gap between BP2(S) and BP2(R) and a predicted ee of 94% for **1e**.

Finally, both ethynyl (**h**) and nitrile (**i**) substituents greatly enhance the predicted ee values of these catalysts in comparison to the unsubstituted cases and lead to uniformly high predicted ee values across all scaffolds, excluding **4**. This was initially confounding, given the different electronic characters of CCH and CN substituents. However, in terms of the electrostatic potential of the catalyst, both ethynyl and nitrile substituents lead to a more favorable electrostatic environment for the formyl C−H group in BP2(R) than in BP2(S) (see Figure 6). Qualitatively, one can understand these interactions in terms of the partially positively charged formyl C−H interacting with the π-bonds in both CCH and CN in BP2(R) but not BP2(S). The net effect is again the widening of the energy gap between these two key TS structures and enhanced ee values in comparison to the unsubstituted catalysts.

While the overall enantioselectivities are relatively similar across these five scaffolds, the distribution of TS energies differ markedly (see Figure 2). For instance, the dense distribution of accessible TS energies for catalysts built on scaffold **1** can be contrasted with the rather sparse spectrum of TS energies for **3**. The latter can be explained by the severe steric demands of the ^{t}Bu groups on scaffold **3**, which render many potential TS structures thermodynamically inaccessible. The ultimate result is that some of the scaffolds provide uniformly higher ee values in comparison to others. For instance, for scaffold **2**, 4 of the 10 catalysts considered have predicted ee values exceeding 95%; for **3**, 5 of 9 catalysts are predicted to provide >95% ee.

DOI: 10.1021/acscatal.6b02366
ACS Catal. 2016, 6, 7948−7955

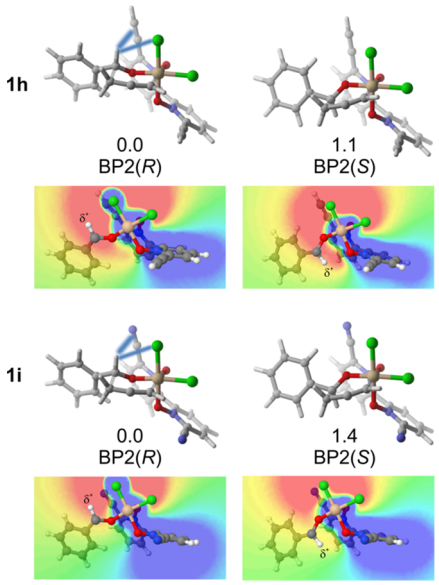

Figure 6. Key TS structures for catalysts **1h,i** along with relative energies in kcal mol^{-1}. The electrostatic potential of the catalyst in the plane of the formyl group of benzaldehyde is also plotted (red, −30 kcal mol^{-1}; blue, +30 kcal mol^{-1}; allenyl group removed for clarity).

The variations in the overall spectrum of TS energies can also have more subtle effects on the ee values, highlighting the importance of considering all accessible TS structures rather than simply the two lowest-lying. For example, catalysts built on scaffold **5** exhibit uniformly higher ee values than the corresponding catalysts built on scaffold **1**. However, in most cases, these enhanced ee values do not arise from changes in the energy gap between BP2(*S*) and BP2(*R*), which are always low-lying for scaffold **5**. Instead, the enhanced ee values result from the destabilization of higher-lying (*S*)-transition states. For example, the energy gap between BP2(*S*) and BP2(*R*) for **5a,b** is the same as that for **1a,b**, respectively. The enhanced enantioselectivites in the former cases derive from the increased energy of the competing ligand configurations (BP1(*S*) and BP3(*S*)), relative to BP2(*R*). For **5c**, the energy gap between BP2(*S*) and BP2(*R*) is actually slightly smaller than for **1c**, and the enhanced enantioselectivity of **5c**, in comparison to **1c**, arises from the destabilization of BP1(*S*) relative to BP2(*R*).

Overall, these data show that the introduction of substituents onto scaffolds **1**−**6** provides broad tuning of predicted ee values in the propargylation of benzaldehyde. However, not all substituents lead to predictable changes in ee values, with some showing marked sensitivity to the choice of catalyst scaffold. Such erratic behavior is disadvantageous from the perspective of rational catalyst design. One constant trend that emerged from these data is that the tuning of the electrostatic environment of the formyl C−H group of benzaldehyde can be used to preferentially stabilize BP2(*R*), providing a potential path to the design of catalysts with high ee values.

Additional Catalyst Design. To explore this strategy of tuning the electrostatic environment of the formyl C−H, we investigated one final catalyst design (**7**; Figure 7). This catalyst features cyclohexene rings fused onto scaffold **1**, which enables the more strategic placement of an electronegative fluorine in close proximity to the formyl C−H. This comes at some cost, however, since the conformational flexibility of these fused rings introduces many additional thermodynamically accessible TS conformers. Moreover, many of these conformers are not

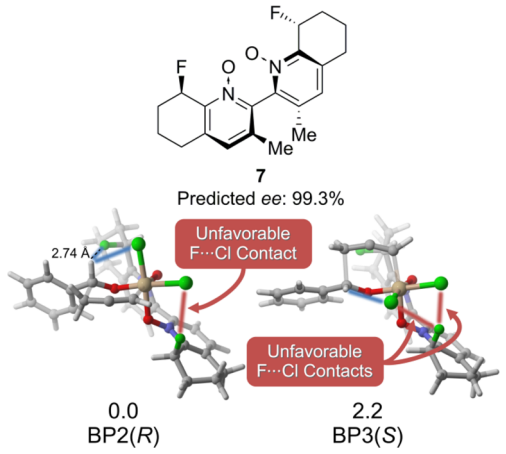

Figure 7. Catalyst **7** along with the key (*R*)- and (*S*)-transition states and relative energies in kcal mol^{-1}.

C_2 symmetric, leading to even more TS structures that must be considered. Regardless, we used AARON to compute all 60 TS structures for a simplified version of **7** (with the Me groups replaced with H). On the basis of these results, we computed all thermodynamically accessible TS structures for catalyst **7**, predicting an ee exceeding 99%. Ultimately, this design is predicted to be as enantioselective as **2e** and **3i**, which were the most enantioselective designs from the initial catalyst library. Notably, the predicted ee for **7** exceeds those of other catalysts with fluoro substituents. In **7**, one of the fluorines is only 2.74 Å from the formyl C−H, providing substantial electrostatic stabilization of BP2(*R*). This distance is shorter than the CH···F distance in either **1b** or **1e**, and the expected electrostatic stabilization of BP2(*R*) is even greater. The result is that BP2(*R*) is 3.0 kcal mol^{-1} lower in energy than BP2(*S*)! However, another consequence is that BP3(*S*) is now lower-lying than BP2(*S*), falling 2.2 kcal mol^{-1} higher in energy than BP2(*R*). It is this (*S*)-transition state that is primarily responsible for the ee of catalyst **7**. The electrostatic environments of the formyl C−H are quite similar in BP2(*R*) and BP3(*S*), and the 2.2 kcal mol^{-1} energy gap can instead be rationalized on the basis of the presence of two unfavorable F···Cl contacts in BP3(*S*), whereas only one such interaction is present in BP2(*R*). Thus, by tuning the electrostatic environment of the formyl C−H group of the benzaldehyde, we were able to significantly increase the energy gap between BP2(*S*) and BP2(*R*). The presence of an additional thermodynamically accessible (*S*)-transition state ultimately limited the overall enantioselectivity.

IV. SUMMARY AND CONCLUDING REMARKS

We have demonstrated the use of DFT to screen a library of potential bipyridine *N,N′*-dioxide catalysts for the asymmetric propargylation of benzaldhyde, identifying 12 catalysts predicted to provide much higher levels of enantioselectivity in comparison to similar catalysts for this reaction.[9b,11b] Notably, many of the catalysts predicted to provide high degrees of enantioselectivity have not previously been synthesized but should be synthetically viable. The synthesis and testing of these catalysts will be highly useful in assessing the reliability of the present predictions. Moreover, we have identified 48 bipyridine *N,N*-dioxide derivatives that are not expected to provide high degrees of enantioselectivities in the propargylation of benzaldehyde; despite this, the synthesis and

DOI: 10.1021/acscatal.6b02366
ACS Catal. 2016, 6, 7948−7955

testing of several of these catalysts would also be highly instructive.

By studying a large number of catalysts for a given asymmetric transformation, we have been able to observe broad trends that would not have been apparent by studying only selected examples. This has provided unprecedented insight into the factors that affect the enantioselectivity of asymmetric propargylations. Overall, we found that the enantioselectivities of these catalysts depend on the interplay of a number of favorable and nonfavorable noncovalent interactions (π-stacking interactions, CH/π interactions, etc.). Ultimately, the most robust means of achieving high ee values is by tuning the electrostatic environment of the formyl C−H of benzaldehyde, which can preferentially stabilize particular TS structures. By exploiting this finding, we were able to design a unique catalyst (7) that is predicted to yield an ee value exceeding 99%.

On the basis of previous computational work on other propargylation and allylation catalysts,[6,11a,12,13] we expect the predicted ee values to be within 10−20% of experiment. However, these predictions come with some caveats. First, we have focused solely on enantioselectivity, with no regard for overall catalytic activity. Potentially, the catalysts predicted to exhibit high degrees of enantioselectivity could prove inactive for the propargylation reaction. Furthermore, for relatively inactive catalysts the background reaction could be competitive, spoiling any predicted enantioselectivity. Similarly, the predicted ee values are based on the implicit assumption that these reactions follow the conventional ionic mechanism[9a,10f,12] and are under Curtin−Hammett control. For some of these catalysts, alternative mechanisms could be viable, invalidating the predicted ee values.

Despite these caveats, the present results demonstrate the feasibility of using DFT to screen a relatively large library of potential organocatalyst designs. This has provided ample experimentally testable predictions. Such a data set, presented prior to the collection of any experimental data, is uncommon and provides a unique opportunity to assess the predictive power of modern quantum mechanical methods. Moreover, these results portend a new design paradigm in which potential organocatalysts are screened computationally, and only the most promising candidates can be synthesized and tested experimentally. Such a strategy would exploit the strengths of both computation and experiment and should ultimately accelerate the development of more effective catalysts. To this end, a new, much more general version of AARON (an automated reaction optimizer for nonmetal-catalyzed reactions) is currently under development.[28]

■ ASSOCIATED CONTENT

Supporting Information

The Supporting Information is available free of charge on the ACS Publications website at DOI: 10.1021/acscatal.6b02366.

Additional data, absolute electronic energies, enthalpies, and free energies, and optimized Cartesian coordinates (PDF)

Cartesian coordinates of the calculated structures (XYZ)

■ AUTHOR INFORMATION

Corresponding Author

*E-mail for S.E.W.: wheeler@chem.tamu.edu.

Present Addresses

†UT Southwestern Medical Center, Dallas, TX, USA.

‡Department of Biostatistics, University of Michigan, Ann Arbor, MI, USA.

§Universal Display Corporation, Ewing, NJ, USA.

Notes

The authors declare no competing financial interest.

■ ACKNOWLEDGMENTS

This work was supported by The Welch Foundation (Grant A-1775) and the National Science Foundation (Grant CHE-1266022). Portions of this research were conducted with high-performance research computing resources provided by Texas A&M University (http://hprc.tamu.edu).

■ REFERENCES

(1) (a) Lam, Y.; Grayson, M. N.; Holland, M. C.; Simon, A.; Houk, K. N. *Acc. Chem. Res.* **2016**, *49*, 750−762. (b) Halskov, K. S.; Donslund, B. S.; Paz, B. M.; Jørgensen, K. A. *Acc. Chem. Res.* **2016**, *49*, 974−986. (c) Sunoj, R. B. *Acc. Chem. Res.* **2016**, *49*, 1019−1028. (d) Reid, J. P.; Simón, L.; Goodman, J. M. *Acc. Chem. Res.* **2016**, *49*, 1029−1041. (e) Peng, Q.; Paton, R. S. *Acc. Chem. Res.* **2016**, *49*, 1042−1051. (f) Wheeler, S. E.; Seguin, T. J.; Guan, Y.; Doney, A. C. *Acc. Chem. Res.* **2016**, *49*, 1061−1069.

(2) (a) Fleming, E. M.; Quigley, C.; Rozas, I.; Connon, S. J. *J. Org. Chem.* **2008**, *73*, 948−956. (b) Houk, K. N.; Cheong, P. H.-Y. *Nature* **2008**, *455*, 309−313. (c) Shinisha, C. B.; Janardanan, D.; Sunoj, R. B. In *Challenges and Advances in Computational Chemistry and Physics*; Leszczynski, J., Ed.; Springer: New York, 2010. (d) Sunoj, R. B. *WIREs Comp. Mol. Sci.* **2011**, *1*, 920−931.

(3) Eksterowicz, J. E.; Houk, K. N. *Chem. Rev.* **1993**, *93*, 2439−2461.

(4) (a) Brown, J. M.; Deeth, R. J. *Angew. Chem., Int. Ed.* **2009**, *48*, 4476−4479. (b) Madarász, Á.; Dènes, B.; Paton, R. S. *J. Chem. Theory Comput.* **2016**, *12*, 1833−1844. (c) Hansen, E.; Rosales, A. R.; Tutkowski, B.; Norrby, P. O.; Wiest, O. *Acc. Chem. Res.* **2016**, *49*, 996−1005. (d) Norrby, P.-O.; Liljefors, T. *J. Comput. Chem.* **1998**, *19*, 1146−1166. (e) Nilsson Lill, S. O.; Forbes, A.; Donoghue, P.; Verdolino, V.; Wiest, O.; Rydberg, P.; Norrby, P.-O. *Curr. Org. Chem.* **2010**, *14*, 1629−1645. (f) Limé, E.; Norrby, P.-O. *J. Comput. Chem.* **2015**, *36*, 244−250. (g) Peña-Cabrera, E.; Norrby, P.-O.; Sjögren, M.; Vitagliano, A.; De Felice, V.; Oslob, J.; Ishii, S.; O'Neill, D.; Åkermark, B.; Helquist, P. *J. Am. Chem. Soc.* **1996**, *118*, 4299−4313. (h) Norrby, P.-O.; Brandt, P.; Rein, T. *J. Org. Chem.* **1999**, *64*, 5845−5852. (i) Norrby, P. O.; Rasmussen, T.; Haller, J.; Strassner, T.; Houk, K. N. *J. Am. Chem. Soc.* **1999**, *121*, 10186−10192. (j) Fristrup, P.; Jensen, G. H.; Andersen, M. L. N.; Tanner, D.; Norrby, P.-O. *J. Organomet. Chem.* **2006**, *691*, 2182−2198. (k) Donoghue, P. J.; Helquist, P.; Norrby, P.-O.; Wiest, O. *J. Chem. Theory Comput.* **2008**, *4*, 1313−1323. (l) Donoghue, P. J.; Helquist, P.; Norrby, P.-O.; Wiest, O. *J. Am. Chem. Soc.* **2009**, *131*, 410−411. (m) Limé, E.; Lundholm, M. D.; Forbes, A.; Wiest, O.; Helquist, P.; Norrby, P.-O. *J. Chem. Theory Comput.* **2014**, *10*, 2427−2435.

(5) Rooks, B. J.; Wheeler, S. E. *AARON:Automated Alkylation Reaction Optimizer for N-Oxides, version 0.72*; Texas A&M University, College Station, TX, 2015.

(6) Rooks, B. J.; Haas, M. R.; Sepúlveda, D.; Lu, T.; Wheeler, S. E. *ACS Catal.* **2015**, *5*, 272−280.

(7) Kobayashi, S.; Nishio, K. *J. Org. Chem.* **1994**, *59*, 6620−6628.

(8) Denmark, S. E.; Coe, D. M.; Pratt, N. E.; Griedel, B. D. *J. Org. Chem.* **1994**, *59*, 6161−6163.

(9) (a) Nakajima, M.; Saito, M.; Shiro, M.; Hashimoto, S.-i. *J. Am. Chem. Soc.* **1998**, *120*, 6419−6420. (b) Nakajima, M.; Saito, M.; Hashimoto, S. *Tetrahedron: Asymmetry* **2002**, *13*, 2449−2452.

(10) (a) Malkov, A. V.; Orsini, M.; Pernazza, D.; Muir, K. W.; Langer, V.; Meghani, P.; Kočovský, P. *Org. Lett.* **2002**, *4*, 1047−1049. (b) Shimada, T.; Kina, A.; Ikeda, S.; Hayashi, T. *Org. Lett.* **2002**, *4*, 2799−2801. (c) Malkov, A. V.; Bell, M.; Orsini, M.; Pernazza, D.;

DOI: 10.1021/acscatal.6b02366
ACS Catal. 2016, 6, 7948−7955

Massa, A.; Herrmann, P.; Meghani, P.; Kočovský, P. *J. Org. Chem.* **2003**, *68*, 9659−9668. (d) Malkov, A. V.; Kočovský, P. *Eur. J. Org. Chem.* **2007**, *2007*, 29−36. (e) Hrdina, R.; Valterová, I.; Hodačová, J.; Císařová, I.; Kotora, M. *Adv. Synth. Catal.* **2007**, *349*, 822−826. (f) Malkov, A. V.; Ramirez-Lopez, P.; Biedermannova, L.; Rulisek, L.; Dufková, L.; Kotora, M.; Zhu, F.; Kočovky, P. *J. Am. Chem. Soc.* **2008**, *130*, 5341−5348. (g) Malkov, A. V.; Westwater, M.-M.; Gutnov, A.; Ramírez-López, P.; Friscourt, F.; Kadlčíková, A.; Hodačová, J.; Rankovic, Z.; Kotora, M.; Kočovský, P. *Tetrahedron* **2008**, *64*, 11335−11348. (h) Hrdina, R.; Dračínský, M.; Valterová, I.; Hodačová, J.; Císařová, I.; Kotora, M. *Adv. Synth. Catal.* **2008**, *350*, 1449−1456. (i) Kadlčíková, A.; Hrdina, R.; Valterová, I.; Kotora, M. *Adv. Synth. Catal.* **2009**, *351*, 1279−1283.

(11) (a) Lu, T.; Porterfield, M. A.; Wheeler, S. E. *Org. Lett.* **2012**, *14*, 5310−5313. (b) Chen, J. S.; Captain, B.; Takenaka, N. *Org. Lett.* **2011**, *13*, 1654−1657.

(12) Sepúlveda, D.; Lu, T.; Wheeler, S. E. *Org. Biomol. Chem.* **2014**, *12*, 8346.

(13) Lu, T.; Zhu, R.; An, Y.; Wheeler, S. E. *J. Am. Chem. Soc.* **2012**, *134*, 3095−3102.

(14) (a) Chelucci, G.; Belmonte, N.; Benaglia, M.; Pignataro, L. *Tetrahedron Lett.* **2007**, *48*, 4037−4041. (b) Hrdina, R.; Opekar, F.; Roithova, J.; Kotora, M. *Chem. Commun.* **2009**, 2314−2316. (c) Sereda, O.; Tabassum, S.; Wilhelm, R. *Top. Curr. Chem.* **2009**, *291*, 349−393.

(15) (a) Becke, A. *J. Chem. Phys.* **1997**, *107*, 8554−8560. (b) Schafer, A.; Huber, C.; Ahlrichs, R. *J. Chem. Phys.* **1994**, *100*, 5829−5835. (c) Grimme, S. *J. Comput. Chem.* **2006**, *27*, 1787−1799.

(16) (a) Cancès, E.; Mennucci, B. *J. Math. Chem.* **1998**, *23*, 309−326. (b) Cancès, E.; Mennucci, B.; Tomasi, J. *J. Chem. Phys.* **1997**, *107*, 3032−3041. (c) Tomasi, J.; Mennucci, B.; Cammi, R. *Chem. Rev.* **2005**, *105*, 2999−3093.

(17) Grimme, S. *Chem. - Eur. J.* **2012**, *18*, 9955−9964.

(18) Frisch, M. J.; Trucks, G. W.; Schlegel, H. B.; Scuseria, G. E.; Robb, M. A.; Cheeseman, J. R.; Scalmani, G.; Barone, V.; Mennucci, B.; Petersson, G. A.; Nakatsuji, H.; Caricato, M.; Li, X.; Hratchian, H. P.; Izmaylov, A. F.; Bloino, J.; Zheng, G.; Sonnenberg, J. L.; Hada, M.; Ehara, M.; Toyota, K.; Fukuda, R.; Hasegawa, J.; Ishida, M.; Nakajima, T.; Honda, Y.; Kitao, O.; Nakai, H.; Vreven, T.; Montgomery, J. A., Jr.; Peralta, J. E.; Ogliaro, F.; Bearpark, M.; Heyd, J. J.; Brothers, E.; Kudin, K. N.; Staroverov, V. N.; Kobayashi, R.; Normand, J.; Raghavachari, K.; Rendell, A.; Burant, J. C.; Iyengar, S. S.; Tomasi, J.; Cossi, M.; Rega, N.; Millam, N. J.; Klene, M.; Knox, J. E.; Cross, J. B.; Bakken, V.; Adamo, C.; Jaramillo, J.; Gomperts, R.; Stratmann, R. E.; Yazyev, O.; Austin, A. J.; Cammi, R.; Pomelli, C.; Ochterski, J. W.; Martin, R. L.; Morokuma, K.; Zakrzewski, V. G.; Voth, G. A.; Salvador, P.; Dannenberg, J. J.; Dapprich, S.; Daniels, A. D.; Farkas, Ö.; Foresman, J. B.; Ortiz, J. V.; Cioslowski, J.; Fox, D. J. *Gaussian 09, Revision D.01*; Gaussian, Inc., Wallingford, CT, 2009.

(19) See ref 12 for a detailed computational study of the enantioselectivity of **4a** for the allylation and propargylation of benzaldehyde.

(20) (a) Lehn, J. M.; Pietraszkiewicz, M.; Karpiuk, J. *Helv. Chim. Acta* **1990**, *73*, 106−111. (b) Lipkowski, J.; Suwinska, K.; Andreetti, G. D. *J. Coord. Chem.* **1990**, *22*, 83−98.

(21) Wheeler, S. E.; Houk, K. N. *J. Chem. Theory Comput.* **2009**, *5*, 2301−2312.

(22) The NPA charges on the formyl C and H are approximately +0.25e and +0.20e, respectively, across all TS structures.

(23) The lowest-lying TS structure is BP1(*R*), which is only 0.1 kcal mol^{-1} lower in energy than BP2(*S*).

(24) (a) Wheeler, S. E. *Acc. Chem. Res.* **2013**, *46*, 1029−1038. (b) Wheeler, S. E.; Bloom, J. W. G. *J. Phys. Chem. A* **2014**, *118*, 6133−6147.

(25) Tauer, T.; Sherrill, C. D. *J. Phys. Chem. A* **2005**, *109*, 10475−10478.

(26) (a) Seguin, T. J.; Wheeler, S. E. *ACS Catal.* **2016**, *6*, 2681−2688. (b) Seguin, T. J.; Lu, T.; Wheeler, S. E. *Org. Lett.* **2015**, *17*, 3066−3069. (c) Seguin, T. J.; Wheeler, S. E. *ACS Catal.* **2016**, *6*, 7222−7228.

(27) The corresponding energy difference is 1.5 kcal mol^{-1} for **1c**.

(28) Guan, Y.; Rooks, B. J.; Wheeler, S. E. *AARON: An Automated Reaction Optimizer for Non-metal catalyzed reactions, version 0.91*; Texas A&M University, College Station, TX, 2016.

DOI: 10.1021/acscatal.6b02366
ACS Catal. 2016, 6, 7948−7955